



In Vitro Study of the Effect of Breathing Pattern on Aerosol Delivery During High-Flow Nasal Therapy

Gavin Bennett · Mary Joyce · Louise Sweeney · Ronan MacLoughlin

Received: December 12, 2018 / Published online: February 6, 2019
© The Author(s) 2019

ABSTRACT

Introduction: The use of concurrent aerosol delivery during high-flow nasal therapy (HFNT) may be exploited to facilitate delivery of a variety of prescribed medications for inhalation. The study assessed the effect of tidal volume, breath rate, and inspiratory:expiratory (I:E) ratio on the quantity of aerosol captured at the level of the trachea during simulated HFNT.

Methods: Testing was completed according to a factorial statistical design of experiments (DOE) approach. Tracheal dose was characterized with a vibrating mesh nebulizer (Aerogen Solo, Aerogen Ltd) using simulated adult, small child, and infant HFNT models. Furthermore, aerosol delivery was evaluated across a range of adult patient profiles with clinically representative test setups.

Results: Aerosol delivery increased with a large tidal volume, a rapid breath rate, and a long inspiratory time. Tidal volume, breath rate, and I:E ratio each had a significant effect on tracheal

dose across simulated adult, small child, and infant breathing.

Conclusion: The main trends that were identified in the statistical DOE predicted aerosol delivery across adult patient breathing profiles, in terms of tidal volume, breath rate, and I:E ratio. Therefore, patients with distressed breathing profiles may be expected to receive a larger aerosol dose than those with normal breathing rates.

Funding: Aerogen Limited.

Keywords: Aerosol; Breathing profile; High-flow nasal therapy; Tracheal dose; Vibrating mesh nebulizer

INTRODUCTION

High-flow nasal therapy (HFNT) is a means of delivering heated humidified air to patient airways that allows for higher flows than conventional low-flow therapy [1]. HFNT provides instantaneous flow rates that equal or exceed inspiratory flow and reduces the inspiratory resistance associated with the nasopharynx [2]. Humidification during HFNT is essential for proper function of the epithelial lining and is an accepted standard of care [3]. Delivering aerosolized medications to the lungs via a nasal cannula interface is particularly advantageous for medications with long delivery times, frequent dosing regimens, or those that require

Enhanced Digital Features To view enhanced digital features for this article go to <https://doi.org/10.6084/m9.figshare.7588862>.

G. Bennett (✉) · M. Joyce · L. Sweeney ·
R. MacLoughlin
Aerogen Limited, IDA Business Park, Dangan,
Galway, Ireland
e-mail: gbennett@aerogen.com

continuous nebulization [4, 5]. The mounting clinical evidence in combination with its ease of use and patient tolerability has resulted in increasing adoption of HFNT, with particular interest in concurrent aerosol delivery during HFNT [6–10]. This includes bronchodilators and mucolytics in chronic and acute episodes of respiratory illness [11]. In vitro studies indicate that aerosols can be efficiently delivered during HFNT [12, 13].

Several factors have been shown to influence the amount of aerosol exiting the cannula during HFNT. These include the rate of gas delivered, size of the nasal prongs, humidification, size of the aerosol droplets, and the type and position of aerosol generator [12–17]. Previously our group reported a systematic approach to determine the conditions required to yield an optimal emitted dose, thus becoming available for inhalation during HFNT [20]. The findings in that study clearly indicate that in order to optimize the amount of aerosol exiting the nasal cannula interface during HFNT, it is necessary for gas flow to be low and the input droplet size to be small, while the nebulizer should be positioned immediately after the humidification chamber [18].

Efficient aerosol delivery to the lungs during HFNT is challenging due to the high velocity gas flows utilized, which may promote preferential aerosol deposition in the nasal passages given the turbulent gas flow in the nose and rhino-pharynx. Furthermore, the nasal passages present a challenge for the aerosols to navigate before reaching the lungs [19–21]. Numerous patient factors may affect the quantity of aerosol available for inhalation during HFNT but to date, few studies have attempted to investigate the effects of breathing pattern on aerosol delivery during this increasingly used patient intervention. Reminiac et al. compared two simulated breathing patterns: quiet breathing and distressed breathing. The respirable mass of drug was significantly higher during simulated respiratory distress compared to simulation of quiet breathing [21]. Dailey et al. [22] showed that with a distressed breathing pattern, aerosol delivery to a filter distal to the cannula was greater at 30 and 50 l/min than with a quiet breathing pattern. Furthermore, breath

simulation has been shown previously to be an accurate in vitro tool for estimating in vivo aerosol delivery [23, 24].

A systematic approach to determine the effects of breathing pattern on the amount of aerosol that could potentially reach the lung during simulated HFNT has not yet been reported. The objective of this study was to address this gap in the literature and determine the effects of tidal volume, breath rate, and I:E ratio on the mass of drug captured at the level of the trachea during simulated HFNT. In addition, and in order to apply these conditions to more physiologically relevant patient scenarios, aerosol delivery was assessed across a range of patient profiles with clinically representative test conditions.

METHODS

Anatomical Models

A previously described airway model of the adult nose–throat region (nasal cavity, pharynx and larynx) based on the nasal cavity of a healthy non-smoking 53-year-old male (weight 73 kg, 173 cm) was used as the adult model [25–27]. A model of a small child nose–throat region (nasal cavity, pharynx and larynx) with a volume of $\sim 22.3 \text{ cm}^3$ is based on a scan of a 5-year-old female, and was used as the small child model [28]. A Sophia anatomical infant nose–throat (SAINT) model based on a scan of a 9-month-old child was used as the infant model, as previously described [29, 30].

HFNT Circuit and Interfaces

The Optiflow™ system (Airvo 2, Fisher and Paykel Healthcare, Auckland, New Zealand) was used. An adult breathing circuit (P/N: 900PT552) was used with an adult nasal cannula (P/N: OPT + 944). A pediatric breathing circuit (P/N: 900PT531) was used with a pediatric nasal cannula (P/N: OPT 318) and an infant nasal cannula (P/N: OPT316). The Airvo 2 system features a humidifier with an integrated flow source and was used in conjunction with a nebulizer adapter. The nebulizer adapter was positioned at the humidification chamber.

Nebulizer

Experiments were performed using the Aerogen Solo, vibrating mesh nebulizer (Aerogen Ltd, Galway, Ireland). The nebulizer performance characteristics, measured using laser diffraction (Spraytec, Malvern Instruments, Malvern, United Kingdom) as previously described [31], are outlined in terms of average droplet size ($3.22 \pm 0.02 \mu\text{m}$ volumetric median diameter) and aerosol output rate ($0.27 \pm 0.02 \text{ ml/min}$).

Design of Experiments

Testing was completed according to a factorial statistical design of experiments (DOE) approach (Minitab 17 Statistical Software, 2010). Experimental runs were created to fit a linear model or a quadratic model, depending on the data generated, in order to establish the conditions necessary to maximize the tracheal dose with adult, small child, and infant breathing patterns. The DOE approach automatically randomized the order in which experimental runs were completed. Thus, the sample number for each experimental run is dictated by the DOE. Testing was performed in accordance with a DOE for adult, small child, and infant breathing patterns. Inputs included tidal volume, breath rate, and I:E ratio. Gas

flows used were as follows: 10 l/min for simulated adult HFNT, 5 l/min for simulated small child HFNT, and 2 l/min for simulated infant HFNT. The input droplet size remained constant for the purposes of the DOE.

Tracheal Dose

Nasal cannulas were positioned in the nose of anatomically relevant nose–throat models, in accordance with manufacturers' instructions (Fig. 1). The nose–throat models were connected to a breathing simulator (Ingmar ASL 5000, Ingmar Medical, Pittsburgh, PA, USA) via a collecting filter (RespirGard II 303, Baxter, Ireland). Tracheal dose was determined by quantifying the mass of drug captured on a filter positioned distal to the trachea. The humidifier was powered on and allowed to come to temperature (37°C) and a 1-ml dose of albuterol sulfate (2 mg/ml) (GlaxoSmithKline Ltd, Dublin, Ireland) was nebulized. Albuterol was used as it is a commonly nebulized formulation used in the characterization of aerosol drug-delivery systems, and is specified for use as a tracer aerosol in the international standard ISO 27427:2013 [32]. At the end of each dose administration, the drug captured on a filter was eluted using 10 ml of deionized water. The mass of drug was quantified by means of UV

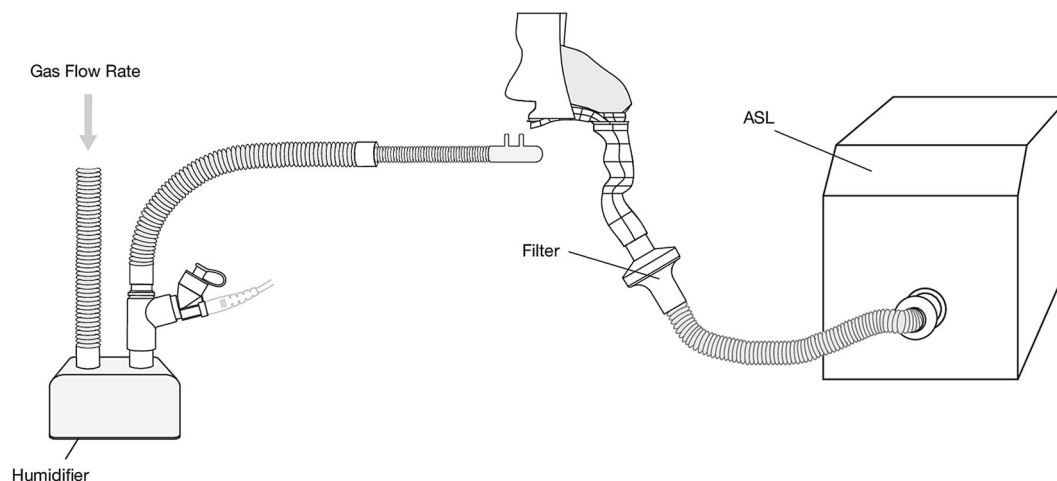


Fig. 1 Illustration of test arrangement employed. High-flow nasal cannulas were positioned on adult, pediatric, and infant head models, which were connected to a

breathing simulator via an absolute filter. The nebulizer was positioned at the humidification chamber

spectrophotometry at a wavelength of 276 nm and interpolation on a standard curve of albuterol sulfate concentrations (200 to 3.125 $\mu\text{g}/\text{ml}$). Results for tracheal dose were expressed as the percentage of the nominal dose placed in the nebulizer's medication cup.

Breathing Profiles

Aerosol delivery was evaluated and compared across a range of adult breathing profiles: normal, distressed, asthma, cystic fibrosis (CF) and acute respiratory distress syndrome (ARDS). Breathing parameters were selected for each patient type based on previously reported studies [23, 33–38] and are outlined in Table 1. It is important to state that airway diseases of this nature have a profound variability depending on severity and acuity of illness. Therefore, the breathing profiles listed should not be considered an absolute, rather an estimate based on parameters independently reported in the literature to date.

Table 1 Breathing parameters used for each adult patient profile

Patient type	Tidal volume (ml)	Breath rate (BPM)	I:E ratio
Normal	500	15	1:2
Distressed	750	30	1:1
Asthma	290	22	1:2.5
CF	429	22	1:2.5
ARDS	475	25	1:2
Reminiac et al. [21] (normal)	500	15	1:1
Reminiac et al. [21] (distressed)	750	30	1:1
Dailey et al. [22] (normal)	500	16	1:2
Dailey et al. [22] (distressed)	750	30	1:1
Reminiac et al. [21] (normal infant)	25	40	1:3

Testing was completed at 50 l/min, in order to simulate a clinically representative set-up. Fifty liters per min is a gas flow that is commonly utilized for HFNT in the hospital setting and has been employed in large multi-center trials designed to assess the clinical utility of HFNT [39]. In order to compare this study with results reported in the literature, research completed by Reminiac et al. and Dailey et al. were replicated.

Statistical Data Analysis

Following the completion of testing according to the statistical DOE approach, a bar graph of standardized effects was generated. If factors in the linear model or the quadratic model reached a 0.10 level of significance, it was concluded that there was a significant relationship between these factors and tracheal dose. Student's *t* tests were performed to determine significant differences in tracheal dose between various adult patient profiles. *P* values of < 0.05 were considered statistically significant (Minitab 17 Statistical Software, 2010).

Compliance with Ethics Guidelines

This article does not contain any studies with human participants or animals performed by any of the authors.

RESULTS

Adult Tracheal Dose

The values of tracheal dose (%) during simulated HFNT using an adult nose–throat model are outlined in terms of mean \pm standard deviation (Table 2). A bar graph of standardized effects was generated by the DOE model (Fig. 2). Tidal volume, breath rate, and I:E ratio were at the 0.10 level of significance, indicating that all three factors had a significant effect on tracheal dose. I:E ratio had the greatest effect on tracheal dose, followed by breath rate, and then tidal volume. Under the test conditions used, the optimal settings to maximize tracheal dose were

Table 2 Tracheal dose [mean \pm standard deviation (%)] for testing completed according to the DOE using adult breathing settings

Breath rate (BPM)	Tidal volume (ml)	I:E ratio	Sample number (<i>n</i>)	Tracheal dose (%)
5	300	1:3	<i>n</i> = 4	11.40 \pm 0.57
		1:1	<i>n</i> = 4	12.89 \pm 1.18
	450	1:1.5	<i>n</i> = 1	18.68
	600	1:3	<i>n</i> = 4	17.61 \pm 0.68
1:1		<i>n</i> = 4	19.50 \pm 1.07	
15	450	1:3	<i>n</i> = 1	20.59
		1:1.5	<i>n</i> = 17	28.24 \pm 1.77
	600	1:1.5	<i>n</i> = 1	30.07
25	300	1:3	<i>n</i> = 4	9.56 \pm 0.12
		1:1	<i>n</i> = 4	29.28 \pm 2.44
	450	1:1.5	<i>n</i> = 1	25.22
	600	1:3	<i>n</i> = 4	18.75 \pm 1.50
1:1		<i>n</i> = 4	28.95 \pm 1.97	

as follows; tidal volume 600 ml, breath rate 19.1, and I:E ratio 1:1.15. The graph also highlights the effect when settings of two factors are changed together. The main area of focus in this study was to establish how changes to a single factor affect the mean of tracheal dose.

Small Child Tracheal Dose

The values of tracheal dose (%) during simulated HFNT using a nose–throat model of a small child are outlined in terms of mean \pm standard deviation (Table 3). A bar graph of standardized effects was generated by the DOE model (Fig. 2). Tidal volume, breaths per minute, and I:E ratio were at the 0.10 level of significance, indicating that all three factors had a significant effect on tracheal dose. Tidal volume had the greatest effect on tracheal dose, followed by I:E ratio and then breath rate. The optimal settings to maximize tracheal dose are

as follows; tidal volume 250 ml, breath rate 40 BPM, and I:E ratio 1:1.

Infant Tracheal Dose

The values of tracheal dose (%) during simulated HFNT using an infant nose–throat model are outlined in terms of mean \pm standard deviation (Table 4). A bar graph of standardized effects was generated by the DOE model (Fig. 2). Tidal volume, breath rate, and I:E ratio were at the 0.10 level of significance, indicating that all three factors had a significant effect on tracheal dose. Based on the results presented, tidal volume had the greatest effect on tracheal dose, followed by I:E ratio, and then breath rate.

Effect of Breathing Profiles on Tracheal Dose

Aerosol delivery was assessed across a range of adult breathing profiles (normal, distressed, asthma, CF, ARDS). Results of tracheal dose deposition (%) for each breathing profile during simulated HFNT at a gas flow of 50 l/min are shown in Table 5 and Fig. 3. All testing carried *n* = 3. Student's *t* tests were performed to determine significance in tracheal dose between each patient type. Tracheal deposition was significantly greater during simulated distressed breathing, in comparison with normal (*P* value = 0.035), Asthma (*P* value = 0.0009), CF (*P* value = 0.0025) and ARDS (*P* value = 0.0016). To compare the results reported in this study to those in the literature, studies completed by Reminiac et al. [21], Dailey et al. [22], and Reminiac et al. [29] were replicated. Results shown in our study were similar to those reported in existing studies in the literature, and are listed in Table 6.

DISCUSSION

This study details a systematic approach to evaluate the effects of breathing pattern on the amount of aerosol that could potentially reach the lung during simulated HFNT. The design of experiments approach provided a robust model,

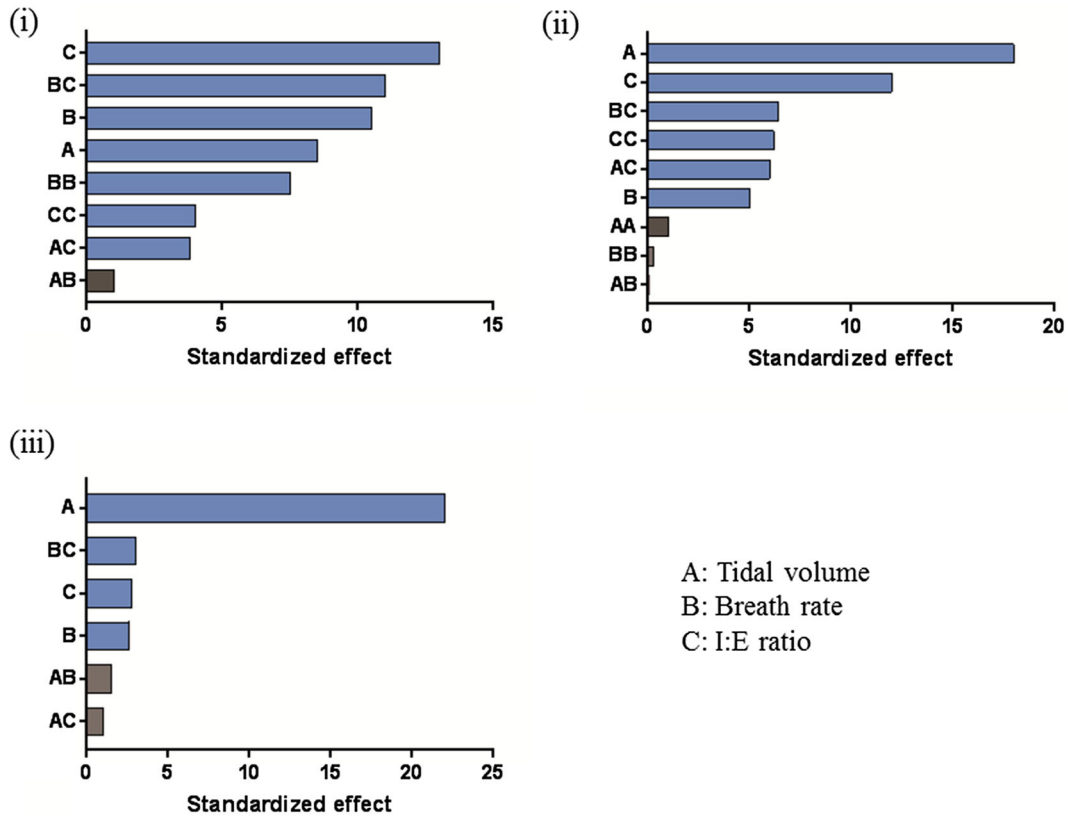


Fig. 2 Effects of tidal volume (a), breath rate (b), and I:E ratio (c) on tracheal dose during simulated adult (i), small child (ii), and infant (iii) breathing. *Blue bars* in the graph show the factors that had a significant effect on the

tracheal dose (at the 0.1 level of significance). *Gray bars* represent non-significant terms that were removed from the model

thus generating usable and representative data without committing to exhaustive testing. Anatomically relevant nose–throat models were utilized to represent airways of adults, small children, and infants, respectively. Aerosol delivery efficiency increased with a large tidal volume, a fast breath rate, and a long inspiratory time. Tidal volume, breath rate, and I:E ratio had a significant effect on tracheal dose across each simulated patient population. In addition, aerosol delivery was assessed in a range of patient profiles with clinically representative test setups. The main trends that were identified in the aforementioned statistical DOE predicted aerosol delivery across patient breathing profiles, in terms of tidal volume, breath rate, and I:E ratio. To the best of our knowledge, this is the first study to evaluate

aerosol delivery across a comprehensive range of patient profiles during simulated HFNT.

Influence of Tidal Volume on Tracheal Dose

Increasing tidal volume was associated with a greater tracheal dose across adult, small child, and infant breathing patterns (Tables 2, 3, 4). This is consistent with several existing studies in the literature for both HFNT and other modes of respiratory drug delivery. Bhasyam et al. [12] showed that aerosol output dose increased from 18.6% with a tidal volume of 150 ml to 25.4% with a tidal volume of 300 ml during simulated HFNT. El Taoum et al. [40] evaluated the delivery of aerosols via the nasal route with face masks in a 7-month and a 5-year-old head

Table 3 Tracheal dose [mean ± standard deviation (%)] for testing completed according to the DOE using small child breathing settings

Breath rate (BPM)	Tidal volume (ml)	I:E ratio	Sample number (n)	Tracheal dose (%)	
20	50	1:3	n = 4	5.60 ± 0.34	
		1:1	n = 4	6.83 ± 0.27	
	150	1:1.5	n = 1	14.78	
		250	1:3	n = 4	12.62 ± 0.48
	30	150	1:1	n = 4	16.40 ± 0.45
			1:3	n = 1	8.46
250		1:1.5	n = 17	13.84 ± 0.42	
		1:1.5	n = 1	16.32	
40	50	1:3	n = 4	6.21 ± 0.24	
		1:1	n = 4	10.64 ± 0.48	
	150	1:1.5	n = 1	15.37	
		25	1:3	n = 4	9.94 ± 0.76
	25	1:1	n = 4	22.85 ± 0.63	

Table 4 Tracheal dose [mean ± standard deviation (%)] for testing completed according to the DOE using infant breathing settings

Breath rate (BPM)	Tidal volume (ml)	I:E ratio	Sample number (n)	Tracheal dose (%)
30	5	1:3	n = 4	4.15 ± 0.88
		1:1	n = 4	3.45 ± 0.89
	50	1:3	n = 4	13.54 ± 0.60
		1:1	n = 4	13.91 ± 2.10
45	27.5	1:1.5	n = 15	9.35 ± 1.03
60	5	1:3	n = 4	2.46 ± 1.17
		1:1	n = 4	4.94 ± 0.94
	50	1:3	n = 4	12.13 ± 0.80
		1:1	n = 4	12.98 ± 1.35

Table 5 Tracheal dose [mean ± standard deviation (%)] for each adult breathing profile

Breathing profile	Tracheal dose (%)
Normal	5.32 ± 0.79
Distressed	9.88 ± 1.00
Asthma	3.73 ± 0.66
CF	5.32 ± 0.59
ARDS	5.29 ± 0.27

model. A higher tidal volume resulted in a greater lung dose for jet nebulizers and vibrating mesh nebulizers. MacLoughlin et al. [41] showed that variation in tidal volume was the most important determinant for aerosol delivery to non-human primates. It is noteworthy that tidal volume was the parameter with the least effect during an adult breathing pattern, but had the greatest effect in small child and infant breathing. This may be due to the differences in dead space across the head models utilized, with tidal volume having a greater influence when models with a lower dead space/smaller airway geometry were employed.

Influence of Breath Rate on Tracheal Dose

A faster breath rate was associated with a greater tracheal deposition across all breathing patterns, with the exception of simulated infant breathing. This is similar to the findings of Reminiac et al. [21]; the respirable mass of drug was significantly higher during simulated respiratory distress. Dailey et al. [22] showed that with a distressed breathing pattern, aerosol delivery was greater at 30 and 50 l/min than with a quiet breathing pattern. This may be due to the increased minute volume (increased tidal volume and breath rate) seen across the distressed pattern, leading to greater aerosol delivery efficiency. In both of these studies, it is difficult to determine the effects of breath rate independently, as tidal volume was altered simultaneously with the breath rate. Here, enabled by the design of the statistical DOE

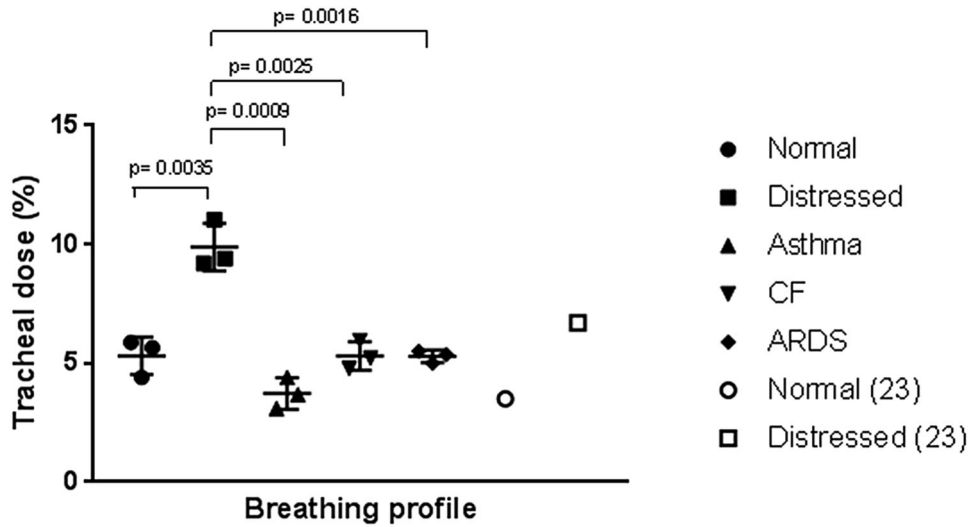


Fig. 3 Illustration tracheal dose [mean \pm standard deviation (%)] for each adult breathing profile. *P* values are included to show significance

Table 6 Results of tracheal dose for a normal and distressed adult breathing pattern (*left*) in comparison with results obtained in previous studies (*right*)

	Normal	Distressed	Normal Reminiac et al. [21]	Distressed Reminiac et al. [21]
30 l/min	9.63	15.02	6.70	10.30
45 l/min	6.20	9.88	3.50	6.70
60 l/min	4.58	7.65	3.00	5.10
	Normal	Distressed	Normal Dailey et al. [22]	Distressed Dailey et al. [22]
10 l/min	19.90	21.76	26.70	13.00
30 l/min	12.08	15.02	11.60	33.00
50 l/min	4.61	11.64	3.50	25.00
	Normal infant		Normal infant Reminiac et al. [21]	
2 l/min	2.08		0.52	
4 l/min	4.36		3.29	
8 l/min	5.27		4.15	

model and the number of test runs completed across each breath rate, authors were enabled to compare breath rate independently while tidal volume and I:E ratio remained constant. For spontaneously breathing adult, small child, and infant breathing patterns, breath rate had a significant effect on aerosol delivery.

Influence of I:E Ratio on Tracheal Dose

A longer inspiratory phase was associated with a greater inhaled dose across all breathing patterns (Tables 2, 3, 4). The optimal I:E ratio was 1:1.15 for simulated adult breathing, 1:1 for simulated small child breathing, and 1:1 for simulated infant breathing. This finding is consistent with that of Bauer et al. who noted a greater inhaled dose with longer inspiratory times in simulated COPD breathing *in vitro*, while using a jet nebulizer. The authors concluded that longer inspiratory times during nebulized drug administration in patients with COPD may lead to increases in the emitted and delivered amount of drug [42]. This may be due to a longer inspiratory time facilitating an increase in aerosol delivery, while losses are minimized with a rapid expiratory phase.

Effect of Breathing Profiles on Tracheal Dose

Tracheal dose was assessed in a range of adult patient profiles across clinically representative test setups. Main trends that were identified in the aforementioned statistical DOE predicted aerosol delivery across patient types, essentially validating the DOE model. Aerosol delivery was significantly greater for simulated distressed breathing in comparison to normal adult, asthma, CF, and ARDS (Fig. 3). The distressed breathing profile had the highest tidal volume, the longest inspiratory time, and the fastest breath rate. This finding is similar to that of Bauer et al. who noted a greater inhaled dose with longer inspiratory times in simulated COPD breathing *in vitro* while using a jet nebulizer [42].

A similar trend was observed when we repeated the study of Reminiac et al. [21]. A

distressed breathing pattern was associated with a greater tracheal dose compared to normal quiet breathing and tracheal dose increased with decreasing gas flow. The tracheal deposition rates that we reported are slightly higher than those noted by Reminiac and colleagues. We hypothesize that these differences are explained by the head models used. We performed testing on an airway model of the adult nose–throat region (nasal cavity, pharynx, and larynx), while Reminiac et al. [21] utilized a thermoplastic polymer nasal cast model. These models may have varying airway geometries. El Taoum et al. [40] showed that the choice of head model significantly affects lung dose.

In relation to the study completed by Dailey et al., we found similar results at 30 l/min and 50 l/min. However, deposition rates reports by Dailey et al. are much higher for distressed breathing. This is most likely due to the fact that no head model was utilized, rather the drug was captured directly on a filter that was positioned distal to the nasal cannula and therefore did not account for deposition losses within the nasal passages of a head model.

In order to replicate the study of Reminiac et al. [29], aerosol delivery was assessed in the same head model: a 9-month-old head model (SAINT). Our results were similar to the findings of that study, where a decrease in aerosol delivery was concurrent with an increasing gas flow.

Study Limitations

It is noteworthy that there were some parameters utilized in the DOE that are not realistic breath settings, for example a breath rate of 5 BPM during simulated adult breathing. Parameters of this nature were employed to provide a broad range for generation of the most appropriate model. Therefore, these were utilized to show trends in aerosol delivery across specific breathing parameters. Subsequent testing detailed tracheal deposition during physiologically relevant breathing profiles with clinically representative test setups.

This article documents aerosol deposition on a filter at the level of the trachea, not the lower

respiratory tract. Usmani and colleagues previously measured regional lung deposition of albuterol in asthmatic subjects, and highlighted the importance of regional targeting for bronchodilator effect [21]. It is vital to emphasize that the difference between tracheal and lower respiratory tract deposition will undoubtedly affect clinical outcomes. However, the intent of this study was to predict the main effects in so far as they could be controlled in a bench model.

CONCLUSIONS

Our findings indicate that a greater tracheal dose was associated with a large tidal volume, a rapid breath rate, and a long inspiratory time. Tidal volume, breath rate, and I:E ratio all had a significant effect on tracheal dose. The main trends that were identified in the statistical DOE predicted aerosol delivery across patient breathing profiles. Furthermore, this is the first study to compare aerosol delivery across a range of breathing profiles during simulated HFNT. This article will be of considerable benefit in increasing the understanding of aerosol delivery during HFNT, an increasingly adopted therapeutic intervention.

ACKNOWLEDGEMENTS

Funding. Funding for the study and article processing charges were provided by Aerogen Limited. All authors had full access to all the data in this study and take complete responsibility for the integrity of the data and accuracy of the data analysis.

Authorship. All named authors meet the International Committee of Medical Journal Editors (ICMJE) criteria for authorship for this article, take responsibility for the integrity of the work as a whole, and have given their approval for this version to be published.

Disclosures. Gavin Bennett is an employee of Aerogen Limited. Mary Joyce is an employee

of Aerogen Limited. Louise Sweeney is an employee of Aerogen Limited. Ronan MacLoughlin is an employee of Aerogen Limited.

Compliance with Ethics Guidelines. This article does not contain any studies with human participants or animals performed by any of the authors.

Data Availability. The datasheets analyzed during the current study are available from the corresponding author on reasonable request.

Open Access. This article is distributed under the terms of the Creative Commons Attribution-NonCommercial 4.0 International License (<http://creativecommons.org/licenses/by-nc/4.0/>), which permits any non-commercial use, distribution, and reproduction in any medium, provided you give appropriate credit to the original author(s) and the source, provide a link to the Creative Commons license, and indicate if changes were made.

REFERENCES

1. Golshahi L, Longest PW, Azimi M, Syed A, Hindle M. Intermittent aerosol delivery to the lungs during high-flow nasal cannula therapy. *Respir Care*. 2014;59(10):1476–86.
2. Dysart K, Miller TL, Wolfson MR, Shaffer TH. Research in high-flow therapy: mechanisms of action. *Respir Med*. 2009;103(10):1400–5.
3. Nava S, Navalesi P, Gregoretti C. Interfaces and humidification for noninvasive mechanical ventilation. *Respir Care*. 2009;54(1):71–84.
4. Walenga RL, Tian G, Hindle M, Yelverton J, Dodson K, Longest PW. Variability in nose-to-lung aerosol delivery. *J Aerosol Sci*. 2014;78:11–29.
5. Dhand R. Aerosol therapy in patients receiving noninvasive positive pressure ventilation. *J Aerosol Med Pulm Drug Deliv*. 2012;25(2):63–78.
6. de Jongh BE, Locke R, Mackley A, Emberger J, Bostick D, Stefano J, et al. Work of breathing indices in infants with respiratory insufficiency receiving high-flow nasal cannula and nasal continuous

- positive airway pressure. *J Perinatol*. 2014;34(1):27–32.
7. Kubicka ZJ, Limauro J, Darnall RA. Heated, humidified high-flow nasal cannula therapy: yet another way to deliver continuous positive airway pressure? *Pediatrics*. 2008;121(1):82–8.
 8. Spentzas T, Minarik M, Patters AB, Vinson B, Stidham G. Children with respiratory distress treated with high-flow nasal cannula. *J Intensive Care Med*. 2009;24(5):323–8.
 9. McKiernan C, Chua LC, Visintainer PF, Allen H. High-flow nasal cannulae therapy in infants with bronchiolitis. *J Pediatr*. 2010;156(4):634–8.
 10. Groves N, Tobin A. High-flow nasal oxygen generates positive airway pressure in adult volunteers. *Aust Crit Care*. 2007;20(4):126–31.
 11. Morgan SE, Mosakowski S, Solano P, Hall JB, Tung A. High-flow nasal cannula and aerosolized beta agonists for rescue therapy in children with bronchiolitis: a case series. *Respir Care*. 2015;60(9):e161–5.
 12. Bhashyam AR, Wolf MT, Marcinkowski AL, Saville A, Thomas K, Carcillo JA, et al. Aerosol delivery through nasal cannulas: an in vitro study. *J Aerosol Med Pulm Drug Deliv*. 2008;21(2):181–8.
 13. Ari A, Harwood R, Sheard M, Dailey P, Fink JB. In vitro comparison of heliox and oxygen in aerosol delivery using pediatric high-flow nasal cannula. *Pediatr Pulmonol*. 2011;46(8):795–801.
 14. Hess DR. Aerosol therapy during noninvasive ventilation or high-flow nasal cannula. *Respir Care*. 2015;60(6):880–93.
 15. Perry SA, Kesser KC, Geller DE, Selhorst DM, Rendle JK, Hertzog JH. Influences of cannula size and flow rate on aerosol drug delivery through the Vapotherm humidified high-flow nasal cannula system. *Pediatr Crit Care Med*. 2013;14(5):e250–6.
 16. Longest PW, Walenga RL, Son Y-J, Hindle M. High-efficiency generation and delivery of aerosols through nasal cannula during noninvasive ventilation. *J Aerosol Med Pulm Drug Deliv*. 2013;26(5):266–79.
 17. Sunbul FS, Fink JB, Harwood R, Sheard MM, Zimmerman RD, Ari A. Comparison of HFNC, bubble CPAP and SiPAP on aerosol delivery in neonates: an in vitro study. *Pediatr Pulmonol*. 2015;50(11):1099–106.
 18. Bennett G, Joyce M, Sweeney L, MacLoughlin R. In vitro determination of the main effects in the design of high-flow nasal therapy systems with respect to aerosol performance. *Pulm Ther*. 2018;4(1):73–86.
 19. Usmani OS, Biddiscombe MF, Barnes PJ. Regional lung deposition and bronchodilator response as a function of beta2-agonist particle size. *Am J Respir Crit Care Med*. 2005;172(12):1497–504.
 20. Heyder J, Gebhart J, Rudolf G, Schiller CF, Stahlhofen W. Deposition of particles in the human respiratory tract in the size range 0.005–15 µm. *J Aerosol Sci*. 1986;17(5):811–25.
 21. Reminiac F, Vecellio L, Heuze-Vourc'h N, Petitcollin A, Respaud R, Cabrera M, Le Pennec D, Diot P, Ehrmann S. Aerosol therapy in adults receiving high-flow nasal cannula oxygen therapy. *J Aerosol Med Pulm Drug Deliv*. 2015;29(2):134–41.
 22. Dailey PA, Harwood R, Walsh K, Fink JB, Thayer T, Gagnon G, et al. Aerosol delivery through adult high-flow nasal cannula with heliox and oxygen. *Respir Care*. 2017;62(9):1186–92.
 23. Bosco AP, Rhem RG, Dolovich MB. In vitro estimations of in vivo jet nebulizer efficiency using actual and simulated tidal breathing patterns. *J Aerosol Med Pulm Drug Deliv*. 2005;18(4):427–38.
 24. Roth AP, Lange CF, Finlay WH. The effect of breathing pattern on nebulizer drug delivery. *J Aerosol Med Pulm Drug Deliv*. 2003;16(3):325–39.
 25. Xi J, Si X, Longest W. Electrostatic charge effects on pharmaceutical aerosol deposition in human nasolaryngeal airways. *Pharmaceutics*. 2014;6(1):26–35.
 26. Longest PW, Golshahi L, Behara SR, Tian G, Farkas DR, Hindle M. Efficient nose-to-lung (N2L) aerosol delivery with a dry powder inhaler. *J Aerosol Med Pulm Drug Deliv*. 2015;28(3):189–201.
 27. Rygg A, Longest PW. Absorption and clearance of pharmaceutical aerosols in the human nose: development of a CFD model. *J Aerosol Med Pulm Drug Deliv*. 2016;29(5):416–31.
 28. https://www.rddonline.com/resources/tools/pediatric_upper_airway_models.php. Accessed 8 Nov 2017.
 29. Reminiac F, Vecellio L, Loughlin RM, Le Pennec D, Cabrera M, Vourc'h NH, et al. Nasal high-flow nebulization in infants and toddlers: an in vitro and in vivo scintigraphic study. *Pediatr Pulmonol*. 2017;52(3):337–44.
 30. Janssens HM, de Jongste JC, Fokkens WJ, Robben SG, Wouters K, Tiddens HA. The Sophia Anatomical Infant Nose-Throat (Saint) model: a valuable tool to study aerosol deposition in infants. *J Aerosol Med Pulm Drug Deliv*. 2001;14(4):433–41.

31. MacLoughlin R, Higgins B, Laffey J, O'Brien T. Optimized aerosol delivery to a mechanically ventilated rodent. *J Aerosol Med Pulm Drug Deliv.* 2009;22(4):323–32.
32. International Organization for Standardization (ISO): Anaesthetic and respiratory equipment—Nebulizing systems and components. 2013.
33. Fadda E, Galimberti E, Cammino S, Bellodi L. Smoking, physical activity and respiratory irregularities in patients with panic disorder. *Rivista di psichiatria.* 2013;48(4):293–300.
34. Arnal J-M, Garnero A, Novonti D, Demory D, Ducros L, Berric A, et al. Feasibility study on full closed-loop control ventilation (IntelliVent-ASVTM) in ICU patients with acute respiratory failure: a prospective observational comparative study. *Crit Care.* 2013;17(5):R196-R.
35. Kondili E, Alexopoulou C, Xirouchaki N, Vaporidi K, Georgopoulos D. Estimation of inspiratory muscle pressure in critically ill patients. *Intensive Care Med.* 2010;36(4):648–55.
36. Officer TM, Pellegrino R, Brusasco V, Rodarte JR. Measurement of pulmonary resistance and dynamic compliance with airway obstruction. *J Appl Physiol.* 1998;85(5):1982–8.
37. Volsko TA, Hoffman J, Conger A, Chatburn RL. The effect of targeting scheme on tidal volume delivery during volume control mechanical ventilation. *Respir Care.* 2012;57(8):1297–304.
38. Kondili E, Alexopoulou C, Prinianakis G, Xirouchaki N, Georgopoulos D. Pattern of lung emptying and expiratory resistance in mechanically ventilated patients with chronic obstructive pulmonary disease. *Intensive Care Med.* 2004;30(7):1311–8.
39. Frat JP, Thille AW, Mercat A, Girault C, Ragot S, Perbet S, et al. High-flow oxygen through nasal cannula in acute hypoxemic respiratory failure. *N Engl J Med.* 2015;372:2185–96.
40. El Taoum KK, Xi J, Kim J, Berlinski A. In vitro evaluation of aerosols delivered via the nasal route. *Respir Care.* 2015;60(7):1015–25.
41. MacLoughlin RJ, Van Amerongen G, Fink JB, Janssens HM, Duprex PW, De Swart RL. Optimization and dose estimation of aerosol delivery to non-human primates. *J Aerosol Med Pulm Drug Deliv.* 2016;29(3):281–7.
42. Bauer A, McGlynn P, Bovet LL, Mims PL, Curry LA, Hanrahan JP. The influence of breathing pattern during nebulization on the delivery of arformoterol using a breath simulator. *Respir Care.* 2009;54(11):1488–92.